Answer to Reviewer #2:

There is no doubt, that the rainfall shows a "parabolic pattern", however, after showing the individual datapoints in fig.3 the former point cloud now shows linear declines of CO2 flux for each site. Therefore, I assume that the autors mean by "parabolic pattern" a maximum CO2 flux which is limited by a parabolic function? If that is the case, I recommend that the authors include a parabolic function into Fig. 3 and better describe what "parabolic pattern" actually means to them. Otherwise, I recommend to discuss the linear decline with existing literature, Skopp et al. 1990.

In response to this comment, we have now shown the parabolic curve on Figure 3 and included the equation, R-squared and P-value in the figure heading (Lines 38-40). Although it may not be clear on the scatterplot, if we showed linear regressions for the individual sites, these would in fact show an increase of CO2 with soil moisture. However, remember that we are using these sites as a surrogate variable to represent a range of soil conditions, and as such we want to look at the relationship across sites; this relationship was parabolic, as we now show in Figure 3 and have observed previously in Panama (Koehler et al. 2009, fig. 3), in Indonesia (van Straaten et al. 2011, fig. 5), in Costa Rica (Schwendenmann et al. 2003, fig. 3), and in Brazil (Sotta et al. 2006, fig.4).

My intention was not to motivate the authors for including a sentence about using microbial abundance and activity in future studies, but rather to discuss their findings in a better context to microbial processes. As I learned from the replies to R1, there is another paper on its way which might deal with that topic? However, also this paper would highly benefit if the coupling of CH4 and N2O fluxes would be discussed. I agree that denitrification is not making sense. However, especially in the dry season when CH4 uptake is dominant and soils are more oxic, also denitrification should be decreased. Since methanotrophs are also known to produce N2O, the decrease of N2O caused by denitrification might be larger than the increase of N2O caused by methanotrophy and therefore no clear correlation between CH4 and N2O is obtained.

Yes, there is an N-cycling paper planned. For this paper, we agree that a discussion of the coupling of CH4 and N2O fluxes would have been really interesting if our results had supported such a discussion. However, there was simply no evidence of this relationship based on our correlation analysis, quite possibly for the reasons suggested in this comment. To incorporate that idea into our discussion, we have now expanded the first paragraph of Section 4.5 (Lines 606-612) to note that we may have missed correlations between gross production/consumption processes belowground, as we were only measuring net fluxes at the soil surface.

I agree that the ambient NO mixing ratio is not the right one to use in a scatter plot, however, I would use the NO mixing ratio shortly before reopening the chamber. Also I think it might be worth to include a statement about potential effects of a variable NO background (before closing and after opening the chamber) on the NO flux measured in between.

We disagree that it would be better to use the NO mixing ratio inside the chamber, particularly during the period shortly before reopening it, as the NO concentration at that time is already the net effect of the chemical reaction (deposition onto the soil within the chamber through reaction

of ambient NO with ambient O_3; Pape et al. 2009) and microbiological processes (NO consumption in the soil as an intermediate product of nitrification and denitrification; Davidson et al. 2000). That would not support our discussion of how the net NO flux was driven by the ambient NO concentration as well as the NO production/consumption capacity of the soils across those periods of measurements. Regarding the variable NO background, this is shown in Figure 5 (i.e. the relationship between ambient NO concentration and soil NO flux) and is discussed extensively in the revised version of Section 4.4, with the dialogue concerning the chemical reactions/microbiological processes resulting in net negative NO fluxes (see Lines 565-580 in Section 4.4 of the manuscript).

Answer to the Subject Editor:

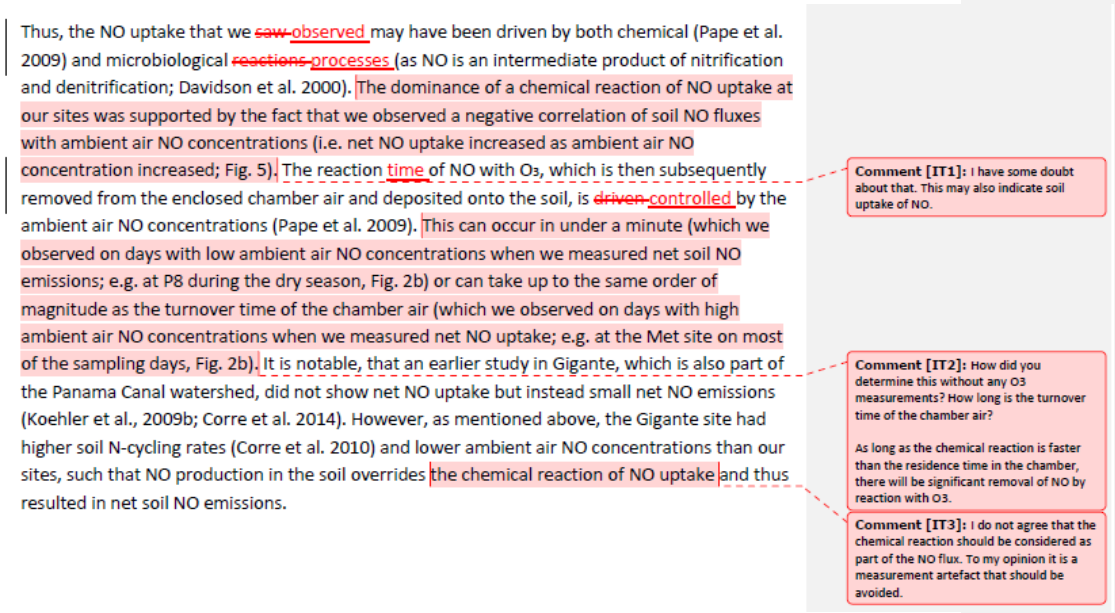

Comment 1: We have incorporated this comment into the revised last sentence of Lines 565-580 by not claiming the 'dominance' of chemical reaction of NO over that of microbially-mediated NO consumption in the soil.

Comment 2: We decided to delete this sentence in the revised version as this is actually not necessary to support our argument. However, in answer to this question: we calculated the turnover time of the enclosed chamber air by chamber vol. (11 L) ÷ sampled air flow rate (0.5-0.6 L/min) (Lines 178 & 182). This statement was based on our results which we included during the initial review (see below Fig. 1a-b).

Comment 3: We agree that NO 'uptake' may not be the best term to use, so in the Results section we include both terms (previous line 388 now reads 'In all five sites, net NO uptake or negative NO flux ….') and then throughout the manuscript we now use 'net negative NO flux'. However, we disagree that the reaction of ambient NO with ambient O_3 within the chamber prior to the measurement system (where the sampled gas is passing through the CrO_3 – luminol – detector) should be termed a measurement artifact. This principle of NO measurement by Scintrex LMA-3 chemiluminescence is an established method for field studies in the tropics that have used the dynamic chamber method (Veldkamp et al. 1998, Verchot et al. 1999, Hall and Matson 2003, Keller et al. 2005, Purbopuspito et al. 2006, Koehler et al. 2009; Hassler et al. 2017). The reaction of NO with ambient O_3 normally happens within a few seconds after chamber closure (see Fig 1a), and hence is usually overshadowed by the linear change of NO concentrations during the 5- to 7-minute measurement of chamber closure. We observed such long reactions of ambient NO with O3 within the chamber (see Fig. 1b) during periods and/or in sites that had high O3 concentrations due to the proximity to O3 sources. Thus, it is not the measurement method but the unusually high O3 concentrations that led to net negative NO fluxes. Therefore, instead of terming these negative NO values as measurement artifacts, we include in our revised discussion that these negative NO fluxes are caused by both chemical and microbiological reactions.

<u>Other changes made in this version:</u>

Line 10: contact email for A. Matson was updated

Line 66/439: spelling mistake in author name corrected

Line 160/177: terminology standardized for chamber methods (using 'vented' in both cases)

Table 4: changed formatting to match the other tables

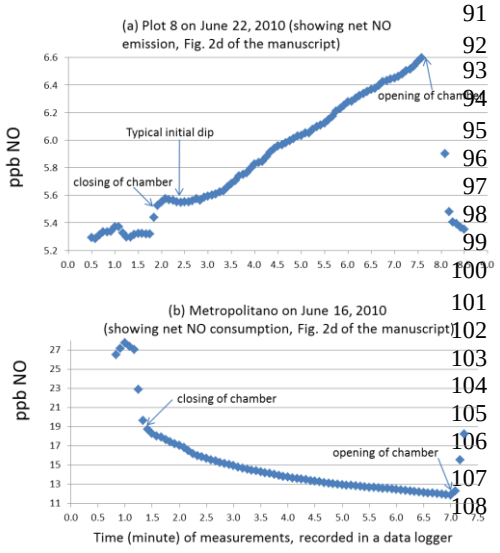

Fig. 1. Typical measurements depicting net NO emission (usually occurred when ambient NO concentration was low) and net negative NO flux (usually occurred when ambient NO concentration was high).

Soil trace gas fluxes along orthogonal precipitation and soil fertility gradients in tropical lowland forests of Panama

Amanda L. Matson[*1], Marife D. Corre[*1], Kerstin Langs[1] and Edzo Veldkamp[1]

[*]These authors contributed equally to this work

[1]Soil Science of Tropical and Subtropical Ecosystems, Büsgen Institute, University of Goettingen, Buesgenweg 2, 37077, Goettingen, Germany

Correspondence to: Amanda L. Matson (~~amatson@gwdg.de~~amanda.matson@scionresearch.com)

Abstract

Tropical lowland forest soils are significant sources and sinks of trace gases. In order to model soil trace gas flux for future climate scenarios, it is necessary to be able to predict changes in soil trace gas fluxes along natural gradients of soil fertility and climatic characteristics. We quantified trace gas fluxes in lowland forest soils at five locations in Panama, which encompassed orthogonal precipitation and soil fertility gradients. Soil trace gas fluxes were measured monthly for one (NO) or two (CO_2, CH_4, N_2O) years (2010-2012), using vented dynamic (for NO only) or static chambers with permanent bases. Across the five sites, annual fluxes ranged from: 8.0 to 10.2 Mg CO_2-C ha^{-1} yr^{-1}, -2.0 to -0.3 kg CH_4-C ha^{-1} yr^{-1}, 0.4 to 1.3 kg N_2O-N ha^{-1} yr^{-1} and -0.82 to -0.03 kg NO-N ha^{-1} yr^{-1}. Soil CO_2 emissions did not differ across sites, but did exhibit clear seasonal differences and a parabolic pattern with soil moisture across sites. All sites were CH_4 sinks; within-site fluxes were largely controlled by soil moisture whereas fluxes across sites were positively correlated with an integrated index of soil fertility. Soil N_2O fluxes were low throughout the measurement years, but highest emissions occurred at a mid-precipitation site with high soil N availability. Net negative NO fluxes at the soil surface ~~uptake in the soil~~ occurred at all sites, with the ~~highest uptake~~most negative fluxes at the low-precipitation site closest to Panama City; ~~NO uptake~~this was likely due to high ambient NO concentrations from anthropogenic sources. Our study highlights the dual importance of short-term (climatic) and long-term (soil/site characteristics) factors in predicting soil trace gas fluxes.

Keywords: greenhouse gases, carbon dioxide, methane, nitric oxide, nitrous oxide, tropical forest

1 Introduction

Soils can be both sources and sinks of carbon dioxide (CO_2), methane (CH_4), nitrous oxide (N_2O) and nitric oxide (NO). Tropical forest soils, specifically, are the largest natural source of soil CO_2 (Raich and Schlesinger, 1992) and N_2O (Bouwman et al., 1993; Prather et al., 1995) and can be significant sinks of CH_4 (Steudler et al., 1996; Keller et al., 2005; Sousa Neto et al., 2011). Although soil NO fluxes in tropical forests are often low (Keller and Reiners, 1994; Koehler et al., 2009b), and the canopy can act as a sink for a large proportion of soil-emitted NO (Rummel et al., 2002), even low emissions may be important in regulating atmospheric oxidant production (Keller et al., 1991; Chameides et al., 1992). However, annual soil trace gas fluxes in Central and South American (CSA) tropical lowland forests can vary significantly; in one study, N_2O emissions varied by one order of magnitude (1.23 to 11.39 kg N ha^{-1} yr^{-1}; Silver et al., 2005). Such disparity in measurements, caused by the temporal and spatial variability found in tropical forests (Townsend et al., 2008), makes it challenging to model soil trace gas fluxes from these areas and to predict how they might be affected by climate change.

Temporal variations in soil trace gas fluxes are primarily correlated with temperature and moisture. Temperature is often more important where there are annual extremes in temperature - such as in temperate and boreal regions - whereas precipitation and soil moisture are more important in tropical regions, where air temperature does not vary much throughout the year (Saikawa et al., 2013). Soil moisture affects microbial activity both directly through water availability and indirectly through its influence on the soil oxygen status and gas diffusivity (Davidson and Schimel, 1995). Spatial variations in soil trace gas fluxes are largely controlled by soil characteristics. Soil texture, for example, strongly influences soil water retention and gas diffusivity (Koehler et al. 2010; Hassler et al. 2015) as well as soil fertility, plant productivity,

decomposition and ultimately soil nutrient availability (Silver et al., 2000; Sotta et al., 2008; Allen et al., 2015).

Soil CO_2 fluxes at the soil surface are the result of interacting belowground processes, including autotrophic (root) respiration and heterotrophic (microbes and soil fauna) respiration (Raich and Schlesinger, 1992; Hanson et al., 2000). Although temporal and spatial drivers may be affecting these processes differently, the net response of soil CO_2 fluxes shows some consistent trends. Soil CO_2 emissions from CSA tropical forest soils generally exhibit positive relationships with soil temperature (Chambers et al., 2004; Schwendenmann and Veldkamp, 2006; Sotta et al., 2006, Koehler et al., 2009a) and soil moisture (Davidson et al., 2000). The relationship between CO_2 and moisture is often parabolic, with emissions increasing until the threshold at which anaerobic conditions start to inhibit soil CO_2 production and/or gas diffusion and then decreasing (Schwendenmann et al., 2003; Sotta et al., 2006; Koehler et al., 2009a). Spatial differences in soil CO_2 emissions can be affected by soil characteristics. Both Silver et al. (2005) and Sotta et al. (2006) noted a soil texture effect on net soil CO_2 emissions; higher emissions occurred in sandy as compared to clayey Ferralsol soils, which were attributed to respiration from the higher fine root biomass in the sandy soils. Soil fertility can also affect net soil CO_2 emissions; Schwendenmann et al. (2003) observed a positive relationship between soil CO_2 flux and spatial differences in soil organic C and total N, and a negative relationship with soil total P (possibly due to lower fine root biomass in areas of high P).

Soil CH_4 fluxes reflect the combined activity of both methanotrophs (CH_4 consumers) and methanogens (CH_4 producers), the ratio of which can change in space and time. Since the activity of both functional groups can increase with temperature (Conrad, 1996; Chin et al., 1999; Mohanty et al., 2007), net changes of soil CH_4 fluxes in response to temperature are more likely to be driven

by other site conditions, such as soil moisture. Soil CH_4 fluxes (predominant flux indicated by positive values (net emissions) or negative values (net consumption)) in CSA tropical lowland forests often exhibit positive correlations with soil moisture (Keller and Reiners, 1994; Verchot et al., 2000; Davidson et al., 2004; Veldkamp et al., 2013) since high soil moisture conditions favor CH_4 production, while CH_4 consumption is reduced due to inhibited diffusion of CH_4 from the atmosphere to the soil (Le Mer and Roger, 2001; Koehler et al., 2012; Veldkamp et al., 2013). Although they have less often been the focus of CH_4 studies, soil biochemical characteristics (i.e. soil fertility status) may also play an important role. Veldkamp et al. (2013) reported that increases in soil N availability stimulate CH_4 uptake and/or reduce CH_4 production in soil, and Hassler et al. (2015) also showed that soil fertility (i.e. increased soil N availability and decreased soil exchangeable Al) enhances soil CH_4 uptake.

N-oxide gases (N_2O and NO) are produced and consumed through the microbial processes of nitrification and denitrification (Chapuis-Lardy et al., 2007). In general, soil NO production through nitrification dominates in aerobic conditions whereas soil N_2O production through denitrification dominates in anaerobic conditions (Conrad, 2002). Therefore, as shown in several CSA tropical forest studies (Keller and Reiners, 1994; Verchot et al., 1999; Davidson et al., 2004; Keller et al., 2005; Koehler et al., 2009b), with increases in soil moisture, soil NO fluxes generally decrease (though Gut et al., 2002 show that this relationship is complex) while soil N_2O fluxes increase. Soil temperature can also be positively correlated with NO flux (Gut et al., 2002), and negatively correlated with soil N_2O emissions (Keller et al., 2005), though this may be due to a co-correlation of soil temperature with soil moisture. Soil N-oxide fluxes may also be affected by soil texture; soil N_2O emissions can be stimulated by the higher soil N availability and greater proportion of anaerobic microsites in clayey soils (Keller et al., 2005; Silver et al., 2005; Sotta et

al., 2008) whereas soil NO fluxes can be facilitated by the higher diffusivity in sandy soils (Silver et al., 2005). Finally, as an essential substrate for nitrification and denitrification, N availability in the soil is a primary controlling factor of soil N-oxide fluxes (Koehler et al., 2009b; Corre et al., 2014).

Climate scenarios suggest that tropical regions may experience large changes in precipitation regimes in the future, with moist tropical regions likely experiencing both higher annual precipitation and more extreme precipitation events (Stocker et al., 2013). Such changes could significantly alter current soil trace gas fluxes, since soil moisture – as described above – plays an important role in both the temporal and spatial variability of soil trace gas fluxes. One approach to studying how changes in precipitation may alter soil trace gas fluxes is to investigate these fluxes along a natural gradient of climate (e.g. precipitation) in a localized region. This approach was used by Holtgrieve et al. (2006) on the Kula volcanic series lava flow in Hawaii, to show that soil N cycling and N-oxide fluxes were strongly affected by mean annual precipitation. However, as suggested by Santiago et al. (2005), precipitation gradients in continental tropical forests, where there are variations in species composition and soil parent material, may exhibit different patterns than those from Hawaii. Additionally, precipitation (or climate) is itself a soil forming factor (Jenny, 1945), and continental tropical lowland soils are considerably older than the relatively young volcanic soils (i.e. Santiago et al., 2005). Therefore, soils of continental precipitation gradients will reflect both the long-term effects of the precipitation regime (i.e. on differences in soil physical and biochemical characteristics) in addition to short-term effects (i.e. on soil moisture).

In this study, we quantified soil trace gas fluxes in tropical lowland forests of the Panama Canal Watershed, spanning a precipitation gradient of 1700-3400 mm yr^{-1} (Figure S1). Soil fertility

(based on an aggregate index that included clay content, ^{15}N natural abundance, effective cation exchange capacity (ECEC), organic C:N ratio, and exchangeable Al; see 2.4) varied orthogonally with this precipitation gradient (Figure S2). The objectives of our study were to: (1) determine how soil fluxes of CO_2, CH_4, N_2O and NO vary along orthogonal gradients of precipitation and soil fertility, and (2) assess and compare the spatial and temporal controls of soil trace gas fluxes in lowland tropical forests. By using orthogonal gradients of precipitation and soil fertility, we were able to examine the relative importance of climatic factors vs. soil biochemical characteristics for soil trace gas fluxes. We hypothesized that the temporal and spatial patterns of soil trace gas fluxes across sites would follow the pattern of the most important controlling soil factors: soil CO_2 fluxes would be parabolic in relation to increasing soil moisture along the precipitation gradient; soil CH_4 fluxes would increase (or CH_4 consumption would decrease) with increasing soil moisture and decreasing soil fertility along the precipitation gradient; and soil NO fluxes would decrease whereas soil N_2O fluxes would increase with increasing soil moisture along the precipitation gradient.

2 Methods

2.1 Study sites

Soil trace gas fluxes were measured in five study sites of the Center for Tropical Forest Science (CTFS) located in the Panama Canal Watershed, central Panama (Table 1; Figure S1). Mean annual air temperature is 27 °C (Windsor, 1990); the soil temperature across all sites fluctuated between 22.5 and 27.5 °C during our study years (Fig. 1a). The five sites span a gradient of annual precipitation from 1700 mm yr^{-1} in Metropolitan National Park (Met) on the Pacific side to 3400 mm yr^{-1} in P32 on the Atlantic side; the dry season generally lasts from January through April

(Corre et al., 2014). The sites were located in either old growth (P8 and P32) or mature secondary (Met, P27, and P19) lowland forests, with tree densities (≥10 cm diameter at breast height, DBH) of: 322 stems ha^{-1} in Met, 395 stems ha^{-1} in P27, 560 stems ha^{-1} in P8, 520 stems ha^{-1} in P19, and 537 stems ha^{-1} in P32 (Pyke et al., 2001). Since precipitation and parent materials vary across these sites, soil types also vary from Cambisols (Met and P27) on the Pacific side to Ferralsols (P8, P19, and P32) on the Atlantic side (Table 1). Floristic composition in these sites has been shown to be correlated with both regional precipitation and geology/soil attributes (Pyke et al., 2001). The amounts and forms of soil organic P are strongly controlled by soil properties whereas the proportion of soil organic P to total P is insensitive to the variation in rainfall and soil properties (Turner and Engelbrecht, 2011).

2.2 Soil trace gas flux calculation

Soil CO_2, CH_4 and N_2O fluxes were determined every 2-4 weeks from June 2010 through February 2012 (28-31 sampling dates) using vented static ~~vented~~ chambers. Within each of the five sites, a 20 m grid was placed over a 1 ha area and we randomly chose four 20 m x 20 m replicate plots with a minimum distance of 20 m between plots. In each replicate plot, four permanent chamber bases were installed (0.04 m^2 area and 0.25 m height after inserting 2 cm into the soil) at the ends of two perpendicular 20 m transects that crossed in the plot's center. The total volume of the chamber (with cover) was 11 L. To determine soil trace gas fluxes, chamber covers were placed on the bases and gas samples (100 mL) were taken 2, 12, 22 and 32 min later. Samples were stored in pre-evacuated glass containers with Teflon-coated stopcocks. At the Gamboa field laboratory, gas samples were then analyzed for CO_2, CH_4 and N_2O concentrations using a gas chromatograph (Shimadzu GC-14B, Columbia, MD, USA) equipped with a flame ionization detector (FID), an

electron capture detector (ECD) and an autosampler, the same instrument that was used in our earlier studies (Koehler et al. 2009a, 2009b, 2010, 2012; Veldkamp et al., 2013; Corre et al. 2014). The instrument's detection limits were 50 ppm CO_2, 43 ppb N_2O and 45 ppb CH_4. Gas concentrations were measured by comparing integration peaks with those of three or four standard gases containing increasing concentrations of CO_2, CH_4 and N_2O (Deuste Steininger GmbH, Mühlhausen, Germany).

Soil NO fluxes were determined every 2-4 weeks from June 2010 through June 2011 (18-21 sampling dates) using ~~open~~ vented dynamic chambers (11 L volume) placed for 5-7 minutes on the same permanent bases described above. The NO ambient mixing ratio was measured at a height of 2 m above the ground (prior to each chamber measurement) near to each of the 4 chamber locations at each of the 4 replicate plots per site on each sampling day. To measure NO, the air from the chamber (ambient air) was sampled by a pump with a flow rate of 0.5-0.6 L min^{-1}, passed through a CrO_3 catalyst that oxidizes NO to NO_2, and flowed across a fabric wick that is saturated with a luminol solution. The luminol then oxidizes and produces chemiluminescence, which is proportional to the concentration of NO_2, and is measured with a Scintrex LMA-3 chemiluminescence detector (ScintrexUnisearch, Ontario, Canada). To minimize deposition losses within the sampling system, all parts in contact with the sample gas are made of Teflon (PTFE). To prevent contamination of tubing and analyzers, particulate matter is removed from the sampled air by PTFE particulate filters (pore size: 5 µm). In order to minimize potential changes in catalyst efficiency caused by variations of air humidity, a known flux of ambient air dried by silica gel was mixed to the sampled air to maintain a humidity of ~50 %; the detector was also calibrated in-situ prior to and following chamber measurements, using a standard gas (3000 ppb NO; DeusteSteininger GmbH, Mühlhausen, Germany). The instrument's detection limit was 0.04 ppb

NO/mV; mV is the electrical signal from the produced chemiluminescence.

Soil trace gas fluxes were calculated as the linear change in concentration over time, and were adjusted for air temperature and atmospheric pressure measured during or directly after sampling. To calculate soil NO fluxes, we considered the first 3 minutes of linear change in NO concentrations with chamber closure time. For CO_2, N_2O and CH_4 fluxes, all 3 gases were analyzed in our gas chromatograph sequentially from the same gas sample. Thus, we based our best fit of gas concentration vs. time on the CO_2 concentration increase, as it is the gas with the highest concentration among these 3 gases. We did not observe any evidence of ebullition (e.g. sudden increase of gas concentration during our 30-min chamber closure), and the CO_2 concentration always increased linearly with time of chamber closure, so a linear fit was used for all 3 gases. Zero fluxes and negative fluxes (i.e. for N_2O and CH_4) were all included in our data analysis. Annual soil NO fluxes were calculated using the June 2010-May 2011 measurements and annual soil CO_2 and N_2O fluxes were calculated using the January to December 2011 measurements; annual fluxes were calculated using the trapezoid rule, assuming a linear relationship in fluxes between sampling days (Koehler et al. 2009a, 2009b, 2010; Veldkamp et al., 2013; Corre et al. 2014).

2.3 Soil biochemical characteristics

In each replicate plot after each soil trace gas flux measurement, samples of the top 5 cm of soil were taken about 1 m from each of the 4 chamber bases, pooled and mixed thoroughly in the field to measure soil extractable NH_4^+ and NO_3^- concentrations and gravimetric water content. In the field, soil samples were placed into prepared extraction bottles containing 150 mL of 0.5M K_2SO_4 and shaken thoroughly. Back at the field station ($\leq$ 6 h after samples were taken), the extraction bottles were again shaken (~ 1 h) and then the extracts were filtered and frozen immediately. The remaining soil was oven-dried at 105 °C for 1 day in order to ascertain gravimetric water content;

this was then used to calculate the dry mass of the soil that had been extracted for mineral N. The frozen extracts were sent by air to the University of Göttingen, Germany for analysis by continuous flow injection colorimetry (Cenco/Skalar Instruments, Breda, Netherlands). The Berthelot reaction method was used to determine NH_4^+ (Skalar Method 155-000) and the copper-cadmium reduction method was used to determine NO_3^- (NH_4Cl buffer without ethylenediaminetetraacetic acid; Skalar Method 461-000).

Soil pits were dug in the center of each of the four replicate plots per site and soil samples were taken for the depth intervals of 0-5, 5-10, 10-25 and 25-50 cm. Soil samples were air-dried and sieved through a 2-mm sieve. Natural abundance ^{15}N signatures were determined from the ground soil samples using isotope ratio mass spectrometry (IRMS; Delta Plus, Finnigan MAT, Bremen, Germany). We calculated the δ^{15}Nenrichment factor (ε) using the Rayleigh equation (Mariotti et al., 1981): $\varepsilon = d_s - d_{so} / \ln f$, where d_s is the $\delta^{15}N$ natural abundance at different depths in the soil profile, d_{so} is the $\delta^{15}N$ natural abundance of the reference depth (top 5 cm), and f is the fraction of total N remaining (i.e. the total N concentration at a given depth divided by the total N concentration in the top 5 cm). The use of only surface $\delta^{15}N$ natural abundance values can be limited, given its inherently high spatial variability (i.e. due to vegetation species differences and surface topography). Therefore, we used not only the surface depth but also 4 depth increments to determine the overall natural abundance enrichment factor (ε). The ε value was used as an integrative indicator of soil N availability, as this correlates with internal soil-N cycling rates (Sotta et al., 2008; Baldos et al., 2015). Total organic C and N were measured from the ground soil samples by dry combustion using a CN analyzer (ElementarVario EL; Elementar Analysis Systems GmbH, Hanau, Germany). ECEC was determined from the sieved soil samples by percolating with unbuffered 1M NH_4Cl and measuring the exchangeable element concentrations

(Ca, Mg, K, Mn, Na, Fe and Al) in the percolates using an inductively coupled plasma-atomic emission spectrometer (ICP-AES; Spectroflame, Spectro Analytical Instruments, Kleve, Germany). Base saturation was calculated as the ratio of exchangeable base cations to the ECEC. Soil pH (H_2O) was analyzed from a 1:4 soil-to-water ratio. Particle size distribution of the mineral soil was determined using the pipette method with pyrophosphate as a dispersing agent (König and Fortmann, 1996).

2.4. Soil fertility index

The variation in soil types along our rainfall gradient (Table 1) was paralleled with variations in soil biochemical characteristics (Table 2; see 3.1). Thus, we developed a soil fertility index using principal component analysis (PCA), similar to the approach employed by Swaine (1996); for each site, the index was based on five soil physical and biochemical properties: 1) clay content, which reflects water- and nutrient-holding capacity, 2) ε that signifies long-term soil N status, 3) ECEC and soil C:N ratio, which indicate bioavailability of rock-derived nutrients and soil organic matter, and 4) exchangeable Al, which implies soil chemical suitability. We used the depth-weighted average of these soil parameters (Table 2), measured at various depth intervals in the top 50 cm depth (except for ε that is calculated for the whole depth; see above). The first component factor of this PCA analysis explained 42 % of the variation in these soil characteristics among sites (Figure S2) and the factor scores were used as the quantitative index of soil fertility for each of the four replicate plots per site. This analysis showed that soil fertility of the five lowland forests varied orthogonally with the precipitation gradient (Figure S2).

370 **2.4 Statistical analyses**

371 We note that our statistical tests are based on the four replicate plots in each of the five 1-ha forest
372 sites along these orthogonal gradients of precipitation and soil fertility, and that the sites
373 themselves were not replicated along the gradients. Consequently, our interpretations and
374 conclusions are limited only to these studied sites.

375 Soil trace gas fluxes (based on the average of the four chambers per replicate plot on each
376 sampling day) and the accompanying soil explanatory variables (soil temperature, gravimetric
377 moisture, NH_4^+ concentration and NO_3^- concentration) were tested for normality using Shapiro-
378 Wilk's test; variables with non-normal distributions were square root or log transformed. We then
379 used linear mixed effects models (LMEs) to assess the differences in these repeatedly-measured
380 variables along the orthogonal precipitation and soil fertility gradients, with site and/or season as
381 the fixed effect(s) and sampling days and replicate plots as random effects. If the Akaike
382 information criterion (AIC) showed an improvement in the LME models, we included a first-order
383 temporal autoregressive function to account for the decreasing correlation of measurements with
384 increasing time (Zuur et al., 2009) and/or a variance function (varIdent) to account for
385 heteroscedasticity of fixed-factor variances (Crawley, 2012). To assess the relationships between
386 soil trace gas fluxes and soil explanatory variables, we used the mean values of the four replicate
387 plots on each sampling date, and conducted Pearson correlation tests over the entire sampling
388 period across the five sites and for each site. Lastly, we analyzed the hierarchy of importance of
389 the soil controlling factors of soil trace gas fluxes by selecting the minimal adequate LME model.
390 For this, we used a stepwise model simplification in which each controlling factor was tested
391 against a null model and the soil factor that showed the lowest AIC value was ranked as the most
392 important; the soil factors with the next lowest AIC values were added step-wise into the model if

this significantly improve the model fit. This analysis was conducted on the mean values of the four replicate plots on each sampling date over the sampling period across the five sites and for each site.

For the soil biochemical characteristics measured only once (Table 2), differences in depth-weighted values (for the top 50 cm) among sites were evaluated using one-way analysis of variance followed by a Tukey HSD test. Their relationships with soil trace gas fluxes across the five sites (using annual values and average seasonal values) were tested using Spearman rank correlations. In all statistical tests, differences among sites or between seasons, correlation coefficients and minimal adequate LME models were considered significant at $P \leq 0.05$.

Data analyses were conducted using the R open source software (R Core Team, 2013).

3 Results

3.1 Soil biochemical characteristics

The soil $\delta^{15}N$ natural abundance signatures and ε, which are proxies of the long-term soil N status (i.e. the higher the values, the higher the soil N availability), were lower at the low-rainfall sites (Met and P27) than at one of the mid-rainfall sites (P19) ($P \leq 0.05$; Table 2). Soil organic C was lower at one of the lower-rainfall sites (P27) than at the high-rainfall site (P32) whereas the differences in total soil N among sites paralleled the increase in annual precipitation ($P \leq 0.05$; Table 2). Soil pH, ECEC and exchangeable bases generally showed the opposite trend to that of total soil N – higher values at the low-rainfall sites (with less-weathered soils) than at the mid- and high-rainfall sites (with highly weathered soils) (all $P \leq 0.05$; Tables 1 and 2). Soil exchangeable Al showed the converse pattern to that of exchangeable bases ($P \leq 0.02$; Table 2).

Of the four soil controlling factors that were monitored over time (temperature, moisture,

extractable NH_4^+ and extractable NO_3^-; Fig. 1a-d), only moisture and extractable NO_3^- differed strongly between seasons ($P < 0.01$; Fig. 1b-c; Table 3); soil moisture contents were higher in the wet season than the dry season at all sites, while extractable soil NO_3^- concentrations were lower in the wet season that the dry season at all sites but P19. Temperature and extractable NH_4^+ exhibited between-season differences at only one site each (temperature - P8, extractable NH_4^+ - P27; Table 3). Within each season, all four soil controlling factors differed along the precipitation gradient (all $P < 0.01$ except $P = 0.04$ for extractable NH_4^+ in the wet season; Table 3). Soil temperatures in both seasons were lower at P32 (3400 mm) than at all other sites (not significant at P27 in the dry season), and also lower at P27 (2030 mm) than Met (1700 mm). Soil moisture contents, in contrast, were higher in both seasons at P32 than at the other four sites. Extractable soil NO_3^- concentrations in both seasons were higher at Met and P8 (2360 mm) than at P27, P19 (2690 mm) and P32, and in the wet season, also higher at Met than P8. Extractable soil NH_4^+ concentrations were higher at P32 than Met in both seasons. Across sites, over the 21-month measurement period, soil moisture was inversely correlated with temperature ($r = -0.28$, $P < 0.01$, $n = 145$) and extractable soil NO_3^- ($r = -0.51$, $P < 0.01$, $n = 145$) and directly correlated with extractable soil NH_4^+ ($r = 0.46$, $P < 0.01$, $n = 145$).

3.2 CO_2 fluxes

Although soil CO_2 emissions did not differ among the five sites over the 21-month measurement period ($P = 0.40$; Fig. 2a; Table 3), emissions exhibited a parabolic relationship with soil moisture across sites (Fig. 3) and were higher in the wet season than the dry season at each site ($P \leq 0.05$; Table 3). Over the 21-month sampling period, average daily soil CO_2 emissions from the five sites were correlated with soil moisture ($r = 0.35$, $P < 0.01$, $n = 145$; Fig. 3), soil temperature ($r = 0.46$,

439 $P < 0.01$, n = 145), extractable soil NH_4^+ (r = 0.32, $P < 0.01$, n = 145) and extractable soil NO_3^- (r
440 = -0.21, $P = 0.01$, n = 145); the dominant drivers in the wet season were extractable NH_4^+ followed
441 by temperature, while the dominant drivers in the dry season were moisture, followed by
442 temperature (Table S1). Within individual sites, daily soil CO_2 emissions exhibited negative
443 correlations with extractable soil NO_3^- at Met (r = -0.48, $P = 0.01$, n = 27), P8 (r = -0.39, $P = 0.03$,
444 n = 30), and P32 (r = -0.54, $P < 0.01$, n = 30). Moisture was a dominant driver of CO_2 emissions
445 from soils at all sites, with temperature (P27, P8 and P32) and mineral N (Met, P19 and P32) both
446 playing important roles as well (Table S1).
447 Similar to the relationship observed for average daily fluxes (Fig. 3), the annual soil CO_2
448 emissions (Table 4) also exhibited a parabolic pattern across the five sites of the precipitation
449 gradient: high at the mid-rainfall sites (P8 and P19) and low at both ends of the precipitation
450 gradient (Met and P32). There were no significant correlations between soil CO_2 emissions
451 (neither for annual CO_2 fluxes nor for wet- and dry-season averages) and the soil biochemical
452 characteristics (Table 5; Table S2).
453
454 **3.3 CH_4 fluxes**
455 On average, despite occasional emissions in the wet season (Fig. 2b), the soils in the five sites
456 acted as CH_4 sinks (Tables 3 and 4). Comparing between seasons, soil CH_4 uptake was higher in
457 the dry season than the wet season at all sites ($P \leq 0.05$; Table 3). Moisture was a dominant driver
458 of CH_4 flux in both seasons, but was stronger in the wet season (Table S1). Differences among
459 sites were the same in both seasons; soil CH_4 uptake at P19 (2690 mm) was higher than at Met
460 (1700 mm), P27 (2030 mm) and P32 (3400 mm), and higher at P8 (2360 mm) than at Met ($P \leq$
461 0.05; Table 3). Over the 21-month sampling period, average daily soil CH_4 fluxes from the five

sites were positively correlated (i.e. soil CH_4 uptake decreased) with soil moisture (r = 0.44, P < 0.01, n = 145; Fig. 4a); moisture was also the dominant within-site driving factor at all sites except Met (Table S1). Across sites, mineral N was a significant explanatory factor in both seasons; within sites, this was only reflected in the model at P32 (Table S1) but average daily soil CH_4 fluxes at P8 (r = -0.63, P < 0.01, n = 30), P19 (r = -0.48, P < 0.01, n = 28) and P32 (r = -0.48, P < 0.01, n = 30) also exhibited negative correlations with extractable soil NO_3^- (i.e. soil CH_4 uptake increased as extractable soil NO_3^- increased).

The annual soil CH_4 fluxes (Table 4) were positively correlated (Spearman *rho* = 0.84, P < 0.01, n = 20; Fig. 4b) with the soil fertility index (Figure S2) and negatively correlated with annual precipitation (*rho* = -0.63, P < 0.01, n = 20; Fig. 4c). Of the soil biochemical properties measured once, annual soil CH_4 fluxes were negatively correlated with soil ^{15}N natural abundance and exchangeable Al, and positively correlated with ECEC, base saturation and pH (Table 5). Average seasonal soil CH_4 fluxes exhibited similar correlations (Table S2); it is notable that when correlation analysis was separated by season, correlations with soil ^{15}N natural abundance were stronger in the dry season than the wet season.

3.4 N_2O fluxes

Soil N_2O fluxes differed among sites only in the wet season and not in the dry season (Table 3; Fig. 2c); soil N_2O emissions in the wet season were higher at P8 (2360 mm) than all other sites (P < 0.01). Notably, the model fit also indicated no significant soil factors for the dry season, but did identify NO_3^- as a driving factor across sites in the wet season (Table S1). Within individual sites, moisture was a controlling factor of N_2O emissions at P8, P19 and P32, with NO_3^- availability also important at P19 (Table S1). Comparing between sites, soil N_2O emissions were higher in the wet

season than the dry season at P8 and P19 (2690 mm) ($P < 0.01$; Table 3). These two sites were also the only two to exhibit correlations with soil controlling factors; soil N_2O emissions increased with increases in soil moisture at P8 (r = 0.69, $P < 0.01$, n = 30) and P19 (r = 0.60, $P < 0.01$, n = 28), and decreased with increases in soil NO_3^- concentration at P8 (r = -0.57, $P < 0.01$, n = 30) and P19 (r = -0.38, $P = 0.05$, n = 28). Annual soil N_2O emissions (Table 4) were negatively correlated with clay content (Table 5). Seasonal average soil N_2O emissions were positively correlated with soil ^{15}N natural abundance in the wet season but not in the dry season (Table S2).

3.5 NO fluxes

In all five sites, net uptake of NO or negative NO flux was measured more often than net NO emissions from the soil (Fig. 2d) and net NO uptake was consistently higher ($P \leq 0.05$) in the wet than dry season, except at P19 (2690 mm) where there was no difference between seasons (Table 3). Wet-season soil NO uptake at Met (1700 mm) was larger than all other sites ($P < 0.01$; Table 3), while in the dry season soil NO uptake at P19 was larger than at P8 (2360 mm) and P32 (3400 mm) ($P < 0.01$; Table 3). Over the 13-month measurement period, there were no driving factors significant across sites in the model fit (Table S1) but soil NO fluxes were negatively correlated (i.e. net NO uptake increased) with ambient NO concentration ($r = -0.34$, $P < 0.01$, n = 103; Fig. 5). Within individual sites, –dominant drivers (Table S1) were moisture (P27 and P8) and temperature (P27), with soil NO fluxes at P8 also exhibiting a negative correlation with soil moisture ($r = -0.67$, $P < 0.01$; n = 21) and positive correlation (i.e. net NO uptake decreased) with extractable soil NO_3^- ($r = 0.65$, $P < 0.01$; n = 21). There were no correlations with average seasonal soil NO fluxes in the wet season, but in the dry season average seasonal soil NO fluxes were negatively correlated with clay content across sites (Table S2).

4 Discussion

4.1 CO_2 fluxes

Soil CO_2 emissions from CSA tropical lowland forests, including Brazil (Davidson et al., 2000, Chambers et al., 2004, Silver et al., 2005, Sotta et al., 2006), Puerto Rico (Raich and Schlesinger, 1992), Panama (Kursar 1989, Koehler et al., 2009a; Nottingham et al., 2010) and Costa Rica (Schwendenmann and Veldkamp, 2006), range from 10.8 Mg C ha^{-1} yr^{-1} (Silver et al., 2005) to 39.7 Mg C ha^{-1} yr^{-1} (Sotta et al., 2006). Our annual soil CO_2 emissions (Table 4) were on the lower end of this range. When compared with other studies in lowland forests of Panama, our values were also at the lower end of those reported for Barro Colorado Island (BCI) (estimated at 14.5 Mg C ha^{-1} yr^{-1} in 1986; Kursar 1989) and Gigante (ranging from 13.59 ± 1.34 to 17.12 ± 1.59 Mg C ha^{-1} yr^{-1} between 2006 and 2008; Koehler et al., 2009a), which can, in part, be attributed to inter-annual variation. Soil CO_2 fluxes at Gigante varied by more than 3 Mg C $ha^{-1}yr^{-1}$ between 2006 and 2008 (Koehler et al., 2009a), and fine litterfall, one of the substrates of heterotrophic respiration, also varied by about 2 Mg ha^{-1} yr^{-1} from 1998 to 2008 (with annual averages of 7.7-9.7 Mg ha^{-1} yr^{-1}; Wright et al., 2011). Moreover, our values were comparable with those of a mature secondary forest (P15 site, 7-18 Mg C ha^{-1} yr^{-1} in 2007/2008; Notthingham et al., 2010) close to our P8 and P19 sites (Figure S1). Finally, three of our sites (Met, P27 and P19) were mature secondary forests, with tree densities (particularly at Met and P27; see 2.1) lower than the old growth forests on BCI (Pyke et al., 2001) and Gigante (Koehler et al., 2009a). This may have additionally influenced soil CO_2 fluxes since up to 35 % of CO_2 emissions can be contributed by root respiration (Silver et al., 2005). Interestingly, regardless of the contribution of autotrophic respiration to soil CO_2 fluxes, we did not detect any significant differences in soil CO_2 fluxes among sites, but only found that across our 5 sites the temporal pattern of soil CO_2 fluxes was strongly related

to soil moisture.

Net soil CO_2 emissions responded to changes in climatic factors on a seasonal scale (i.e. higher soil CO_2 fluxes in the wet than dry season at all sites; Table 3) and to daily fluctuations in soil temperature and moisture across the five sites (see 3.2). The hierarchy of importance of the soil factors are shown in Table S1: at each site (except P27) and during the dry season across sites, soil moisture was the most important driving factor, followed by soil temperature, NH_4^+ or NO_3^-, while during the wet season, when soil moisture was sufficient, the most important soil factors were NH_4^+ and soil temperature (Table S1). The higher CO_2 emissions in the wet season were likely due to the alleviation of water competition between decomposers and vegetation; in seasonal tropical forests, litter tends to fall in the dry season, but low soil moisture limits decomposition until the start of the wet season (Yavitt et al., 2004). Other studies from CSA lowland forests have also reported a positive relationship between soil CO_2 emissions and soil temperature (Chambers et al., 2004; Schwendenmann and Veldkamp, 2006; Sotta et al., 2006, Koehler et al., 2009a), and parabolic relationships (Fig. 3) between soil CO_2 emissions and soil moisture (Schwendenmann et al., 2003; Sotta et al., 2006; Koehler et al., 2009a). Additionally, soil CO_2 emissions responded to changes in soil mineral N both on the plot level and across sites (see 3.2). Relationships between soil CO_2 emissions and soil mineral N concentrations have not been reported in other studies, although Schwendenmann et al. (2003) observed that spatial differences in soil total N were positively correlated with soil CO_2 fluxes, and Koehler et al. (2009a) found that chronic N addition decreased soil CO_2 fluxes in a montane tropical forest (although not in a lowland forest). However, the correlations between CO_2 emissions and both NH_4^+ (positive correlation) and NO_3^- (negative correlation) may also simply be reflecting a co-correlation between extractable mineral N and soil moisture (see 3.2).

In support of our hypothesis, we observed that annual soil CO_2 fluxes exhibited a parabolic

556 pattern along the precipitation gradient (Table 4) similar to the relationship seen with the daily
557 emissions and soil moisture (Fig. 3). However, as mentioned above, soil CO_2 efflux did not differ
558 among the five forest sites of this precipitation gradient (Table 3). This lack of differences between
559 sites could be due to similarity of a soil-controlling factor that results in comparably low soil CO_2
560 emissions at all sites. For example, although organic C and total N differed between sites, the soil
561 C:N ratios were comparable along these orthogonal gradients of annual precipitation and soil
562 fertility (Table 2), suggesting that the bioavailability of soil organic matter for heterotrophic
563 respiration may be similar across sites. Additionally, the microbial communities that contribute to
564 heterotrophic respiration may have adapted to the existing differences in substrate quantity (e.g.
565 soil organic C), soil and climatic characteristics between the sites (Tables 2 and 3) and therefore
566 exhibited an overall similar soil CO_2 efflux.
567
568 **4.2 CH_4 fluxes**
569 Our findings show the scale-dependency of environmental controls on soil CH_4 fluxes – the short-
570 term (seasonal) pattern within and across sites were dominantly controlled by soil moisture,
571 temperature and mineral N (Table S1) whereas the long-term pattern based on annual fluxes across
572 sites was largely controlled by soil fertility (Fig. 4b).
573 The control of soil moisture on soil CH_4 fluxes has been shown in several CSA tropical
574 forest studies (Keller and Reiners, 1994; Verchot et al., 2000; Davidson et al., 2004; Veldkamp et
575 al., 2013). This was also observed at our sites, with less CH_4 uptake during periods of high water
576 content (i.e. wet vs. dry season; Table 3), soil moisture being the dominant controlling factor at
577 each site (except Met) and across sites during each season (Table S1), as well as a positive
578 correlation of soil CH_4 fluxes with water content (Fig. 4a). We attribute the dominant role of soil

579 moisture to controlling gas diffusivity from the atmosphere into the soil and/or methanogenic
580 activity during periods of high moisture. Our annual soil CH_4 uptake (Table 4) was within the
581 range of other reported values from Brazil and Panama (Verchot et al., 2000; Davidson et al., 2004;
582 Keller et al., 2005; Silver et al., 2005; Veldkamp et al., 2013). Studies that have measured stronger
583 uptake in CSA lowland forests (up to 4.90 kg C ha^{-1} yr^{-1}; Keller and Reiners, 1994; Steudler et al.,
584 1996; Keller et al., 2005; Sousa Neto et al., 2011) may have had soils with higher gas diffusivity
585 due to lower soil water content and/or lower clay content (see Veldkamp et al., 2013); in our five
586 sites, the two sites with the highest sand content (P8 and P19; Table 1) exhibited the highest soil
587 CH_4 uptake (Tables 3 and 4). In addition to moisture, soil NO_3^- may also have been an important
588 driver of temporal soil CH_4 uptake in our sites; we observed increased CH_4 uptake as NO_3^-
589 concentrations increased in P8, P19 and P32 (see 3.3) and it was a dominant controlling factor
590 across sites in both seasons (Table S1). Although this may have reflected a co-correlation between
591 soil NO_3^- concentration and soil moisture (see 3.1), increasing CH_4 uptake in the soil with
592 increasing mineral N has been observed in tropical forest soils of Australia (Kiese et al., 2003),
593 Panama (Veldkamp et al., 2013) and Indonesia (Hassler et al., 2013). Additionally, our soils
594 exhibited a correlation between annual soil CH_4 fluxes and soil ^{15}N natural abundance signatures
595 (Table 5), the latter being an indicator of soil N availability (Sotta et al. 2008; Arnold et al. 2009;
596 Baldos et al. 2015). When separated by season, the correlation between soil CH_4 fluxes and soil
597 ^{15}N natural abundance was stronger in the dry season than the wet season (Table S2), supporting
598 our claim that soil N availability enhanced CH_4 uptake in soils when gas diffusion was favorable
599 (dry season).

600 The control of soil fertility on the long-term pattern of soil CH_4 fluxes across sites was
601 depicted by a correlation between annual soil CH_4 fluxes and our calculated soil fertility index

(Fig. 4b), which exhibited an opposite pattern to that of annual precipitation (Figure S2). This soil fertility control was supported by the strong correlations of both annual (Table 5) and seasonal (Table S2) soil CH_4 fluxes with ECEC and exchangeable Al, both included in the soil fertility index (Figure S2; see 2.4). The correlations between soil CH_4 fluxes and fertility indicators reflected the site differences in soil biochemical characteristics (Table 2). Specifically, as shown by the strong inverse correlation between soil $\delta^{15}N$ natural abundance signatures and exchangeable cations (Table 5), the positive correlation between soil CH_4 flux and fertility (Fig. 4b) likely reflected the long-term effects of soil development (Tables 1 and 2) - more CH_4 uptake occurred in highly weathered soils with less rock-derived nutrients but high soil N availability (i.e. high $\delta^{15}N$ natural abundance signatures) (Tables 4 and 5). This supports our hypothesis that soil CH_4 uptake reflected the control of soil moisture and N availability across sites along this precipitation gradient. Our results also highlight the importance of considering soil properties - in particular the degree of soil development - rather than simply climatic factors, when predicting/modeling soil CH_4 fluxes on a large scale.

4.3 N_2O fluxes

Our annual soil N_2O fluxes (Table 4) were within the lower end of the range (1.23 - 11.4 kg N ha^{-1} yr^{-1}) reported from other CSA forest studies (Keller and Reiners 1994, Verchot et al., 1999, Keller et al., 2005, Silver et al., 2005). In comparison with other studies from Panama, our N_2O fluxes were similar to those measured from Gigante during dry years (0.5 ± 0.2 kg N ha^{-1} yr^{-1} in 2008–2009 with annual precipitation 5–26 % lower than the 12-year average; Corre et al. 2014) but slightly lower than those measured from the same site during wet years (1.0 - 1.4 kg N ha^{-1} yr^{-1} in 2006–2007 with annual precipitation 5–17 % higher than the 12-year average; Koehler et al.,

625 2009b). The low soil N_2O fluxes at our sites were likely caused by the generally lower soil N
626 availability compared to the Gigante site; the five sites in our present study had an average gross
627 N mineralization rate of 4 ± 1 mg N kg^{-1} d^{-1} in the 2010 wet season (Corre et al. unpublished data),
628 which was significantly lower than those from Gigante (29 ± 6 mg N kg^{-1} d^{-1} in the 2006 wet
629 season; Corre et al. 2010).

630 Inter-annual variation in rainfall and hence soil moisture can also strongly affect soil N_2O
631 emissions (Corre et al., 2014). Our measured soil N_2O emissions exhibited a tendency to be higher
632 in the wet season than the dry season (P8 and P19; Table 3), highest at the mid-rainfall site of P8
633 (which could mean that at the high-rainfall sites N_2O could have been further denitrified to N_2),
634 and were only correlated with the soil ^{15}N natural abundance signatures (as an indicator of soil N
635 availability) in the wet season (Table S2). At the sites (P8 and P19), where N_2O emissions were
636 higher in the wet than dry season and soil NO_3^- levels were lower in the wet than dry season (Table
637 3), the inverse correlation between daily soil N_2O emissions with NO_3^- concentrations over the 21-
638 month measurement period suggests that during the wet season N_2O production could have been
639 high but might have been further denitrified to N_2, and hence resulted in low soil NO_3^-
640 concentrations. Although the reduction of NO_3^- in the wet season could also be caused by reduced
641 nitrification, measurements in our study area (once in the wet and once in the dry season) showed
642 no significant differences between wet and dry seasons across sites nor at each site (Corre et al.
643 unpublished data). Additionally, gross nitrification was correlated with NO_3^- immobilization, but
644 not with DNRA, suggesting that when there was high NO_3^- availability, this was preferably
645 assimilated by the microbial biomass (Corre et al. unpublished data). On the other hand, the soil
646 NO_3^- levels we show in Table 3 were measured repeatedly, parallel to soil trace gas flux
647 measurement, over our 21-month study period. The soil NO_3^- levels (Table 3) therefore reflected

the concurrently occurring NO_3^- production and consumption processes. The argument that these reflect further denitrification to N_2 is supported by our earlier study in Gigante, where nitrification and denitrification contributed equally to soil N_2O emissions during the dry season but denitrification was the main process contributing to soil N_2O emission in the wet season (Koehler et al., 2012; Corre et al. 2014). Our results partly supported our initial hypothesis, in that soil N_2O emissions were highest at the mid-precipitation site (with the highest soil N availability as indicated by ^{15}N natural abundance; Table 2) due to possible reduction of N_2O to N_2 at the high precipitation site.

4.4 NO fluxes

Our annual soil NO ~~uptake~~ fluxes (Table 4) ~~was~~ were considerably lower than other reported NO fluxes, which are usually small net emissions rather than net uptake. Soil NO emissions from Panama, Costa Rica and Brazil range from 0.26 to 7.88 kg N $ha^{-1}yr^{-1}$ (Keller and Reiners 1994, Verchot et al., 1999, Gut et al., 2002, Keller et al., 2005, Silver et al., 2005, Koehler et al., 2009b; Corre et al. 2014). However, the net negative NO fluxes~~uptake~~ that we measured may be reflecting unusually high ambient air NO concentrations in our forest sites as compared to forests from other studies. Although all of our sites were located in mature-secondary or old-growth forests, the forests were located within the Panama Canal watershed, where there is heavy, year-round marine traffic (~13,000 cargo ships in 2011; Hricko, 2012). Furthermore, the highest levels of ~~soil~~ net negative NO ~~uptake~~ fluxes that we measured were in the Met site (Table 4); in addition to being in the vicinity of the Panama Canal, the park is located within the city limits of Panama City, which has a population of approximately 1.6 million people (The World Factbook, 2015). Therefore, elevated ambient air NO concentrations from anthropogenic emissions may be driving the net

negative NO ~~uptake~~ fluxes that we measured. Our instrument cannot measure O_3 concentration, which could be high in these sites influenced by anthropogenic emissions. Thus, the net negative NO ~~uptake~~ fluxes that we ~~saw~~ observed may have been driven by both chemical reactions (deposition onto the soil within the chamber through reaction of ambient NO with ambient O_3; Pape et al. 2009) and microbiological ~~reactions~~ processes (~~as~~ NO consumption in the soil as ~~is~~ an intermediate product of nitrification and denitrification; Davidson et al. 2000). ~~The dominance of a chemical reaction of NO uptake at our sites was supported by the fact that we observed a negative correlation of soil NO fluxes with ambient air NO concentrations (i.e. net NO uptake increased as ambient air NO concentration increased; Fig. 5).~~ The reaction time of NO with O_3, which is then subsequently removed from the enclosed chamber air and deposited onto the soil, is ~~driven~~ controlled by the ambient air NO concentrations (Pape et al. 2009). ~~This can occur in under a minute (which we observed on days with low ambient air NO concentrations when we measured net soil NO emissions; e.g. at P8 during the dry season, Fig. 2b) or can take up to the same order of magnitude as the turnover time of the chamber air (which we observed on days with high ambient air NO concentrations when we measured net NO uptake; e.g. at the Met site on most of the sampling days, Fig. 2b).~~ It is notable, that an earlier study in Gigante, which is also part of the Panama Canal watershed, did not show ~~net~~ negative NO ~~uptake~~ fluxes but instead small net NO emissions (Koehler et al., 2009b; Corre et al. 2014). However, as mentioned above, the Gigante site had higher soil N-cycling rates (Corre et al. 2010) and lower ambient air NO concentrations than our sites, such that NO production in the soil ~~overrides~~ may have compensated the chemical reaction of ambient NO ~~uptake~~ with O_3 and thus resulted in net soil NO emissions. Contrary to this, the negative correlation of soil NO fluxes with ambient NO concentrations observed in our sites (i.e. net negative NO flux increased as ambient air NO concentration increased; Fig. 5)

suggests that NO production in the soil was overshadowed by the chemical reaction of ambient NO with O_3 and thus resulted in net negative NO fluxes.

The general trend across sites did not support our hypothesis regarding soil NO emission, since local conditions of high ambient NO concentrations in the atmosphere had an overriding effect resulting in net NO uptake in soils (Fig. 2d). However, our results indicated that our soils could also be a net source of NO when soil conditions were favourable and/or ambient air NO concentrations were not elevated. We observed that net NO uptake was consistently higher in the wet season than the dry season (Table 3); in the dry season, when aerobic soil conditions prevailed due to low soil moisture contents (Table 3), NO production in the soil may have been more favoured (Conrad, 2002), partly counteracting the chemical reaction of NO removal from the atmosphere and its deposition onto the soil. This is also supported by the negative correlation between dry-season soil NO fluxes and clay contents of the sites (Table S2), suggesting that soil NO fluxes were responding to conditions favourable for NO production. Favourable soil conditions were most visible at P8, which had the highest soil NO emissions (with low ambient air NO concentrations) in the dry season (Table 3; Fig. 2d); soil NO fluxes at this site increased when aerobic soil conditions prevailed (i.e. negative correlation with soil moisture; see 3.5) and increased with substrate availability (i.e. positive correlation with soil NO_3^-; see 3.5).

In summary, although the soils in our study sites can be a net source of NO, particularly during the dry season (Fig. 2d) and in sites where ambient air NO concentrations were low (Fig. 5), most of the time the soils acted as net sink of NO, signifying the importance of soil and vegetation as NO sinks (Jacob and Bakwin, 1991; Sparks et al., 2001) in areas affected by anthropogenic NO sources.

4.5 Implications for climate change

It is notable that, although all four trace gases were strongly correlated with the temporal variation in soil moisture and had clear differences between seasons (Table 3), there were no correlations between the four soil trace gases when looking at the annual fluxes (Table 5) or seasonal averages (Table S2). This lack of correlation ~~is presumably rooted in~~may ~~indicate~~be due to the interaction of other soil/~~ and/or~~ climatic factors with known drivers of soil trace gas production and consumption. It ~~or~~ may also reflect that ~~could also be reflecting that net~~trace gas fluxes at the soil surface are the net result of gross production/consumption processes occurring belowground, where correlations may exist~~are not portraying the belowground gross production/consumption processes of the different functional groups~~; ~~one future direction could be to do an in-depth~~future research might consider including an analysis of the abundance/activity of functional microbial groups along ~~these~~ gradients of precipitation and fertility to better understand relationships between the different trace gases.

We have shown that in the short term, soil trace gas fluxes were largely controlled by soil moisture, with the additional influences of soil temperature and mineral N concentration. However, in the long term and/or over large spatial scales, the degree of soil development and related soil fertility had a strong influence. Additionally, we have shown that even in presently undisturbed forests, gas fluxes can be affected by 'upstream' anthropogenic activities. Therefore, in order to understand and be able to predict soil trace gas fluxes under future climate scenarios, research needs to focus on identifying and predicting interacting effects of soil and site, as well as climatic characteristics, on soil-atmosphere trace gas exchange.

Acknowledgements

Funding for this study was provided by the Deutsche Forschungsgemeinschaft (DFG, Co 749/1-1) and by the Robert Bosch Foundation (Germany) for M.D. Corre's independent research group, NITROF. We gratefully acknowledge Dr. Helene Muller-Landau for hosting us and facilitating access to the field sites. The Smithsonian Tropical Research Institute and ANAM, Panama provided invaluable administrative and technical support. The efforts of the NITROF assistants (Rodolfo Rojas and Erick Diaz), and the SSTSE laboratory technicians in completing the data collection and analyses were much appreciated.

References

Allen, K., Corre, M. D., Tjoa, A. and Veldkamp, E.: Soil nitrogen-cycling responses to conversion of lowland forests to oil palm and rubber plantations in Sumatra, Indonesia, PLoS ONE, 10(7), e0133325, doi:10.1371/journal.pone.0133325, 2015.

Bouwman, A. F., Fung, I., Matthews, E., and John, J.: Global analysis of the potential for N2O production in natural soils. Global Biogeochem. Cy., 7, 557–597, 1993.

Butterbach-Bahl, K., Baggs, E. M., Dannenmann, M., Kiese, R., and Zechmeister-Boltenstern, S.: Nitrous oxide emissions from soils: how well do we understand the processes and their controls? Phil. Trans. R. Soc., 368, 20130122, 2013.

Chambers, J. Q., Tibuzy, E. S., Toledo, L. C., Crispim, B. F., Iguchi, N., dos Santos, J., Araujo, A. C., Kruijt, B., Nobre, A. D., and Trumbore, S. E.: Respiration from a tropical forest ecosystem: partitioning of sources and low carbon use efficiency. Ecol. Appl., 14, S72–S88, 2004.

Chameides, W. L., Fehsenfeld, F., and Rodgers, M. O.: Ozone precursor relationships in the

762 ambient atmosphere. J. Geophys. Res., 97, 6037–6055, 1992.
763 Chin, K. J., Lukow, T., and Conrad, R.: Effect of temperature on structure and function of the
764 methanogenic archaeal community in an anoxic rice field soil. Appl. Environ. Microbiol.,
765 65, 2341–2349, 1999.
766 Conrad, R.: Soil microorganisms as controllers of atmospheric trace gases (H2, CO, CH4, OCS,
767 N2O, and NO). Microbiol. Rev., 60, 609–640, 1996.
768 Conrad, R.: Microbiological and biochemical background of production and consumption of NO
769 and N_2O in soil. In: Trace Gas Exchange in Forest Ecosystems, (eds Gasche R, Papen H,
770 Rennenberg H), Dordrecht, Kluwer Academic Publishers, pp 3–33, 2002.
771 Corre, M. D., Veldkamp, E., Arnold, J., and Wright, S. J.: Impact of elevated N input on soil N
772 cycling and losses in old-growth lowland and montane forests in Panama. Ecology, 91,
773 1715–1729, 2010.
774 Corre, M. D., Sueta, J. P., and Veldkamp, E.: Nitrogen-oxide emissions from tropical forest soils
775 exposed to elevated nitrogen input strongly interact with rainfall quantity and seasonality.
776 Biogeochemistry, 118, 103-120, 2014.
777 Crawley, M. J.: The R book, Chichester: John Wiley, 2012.
778 Davidson, E. A., and Schimel, J. P.: Microbial processes of production and consumption of nitric
779 oxide, nitrous oxide and methane. In: Biogenic trace gases: measuring emissions from soil
780 and water (eds Matson PA, Harriss RC), Blackwell Science, Oxford, pp 327–357, 1995.
781 Davidson, E. A., Verchot, L. V., Cattânio, J. H., Ackerman, I. L. and Carvalho, J. E. M.: Effects
782 of soil water content on soil respiration in forests and cattle pastures of eastern Amazonia.
783 Biogeochemistry, 48, 53–69, 2000.
784 Davidson, E. A., Yoko Ishida, F., and Nepstad, D. C.: Effects of an experimental drought on soil

emissions of carbon dioxide, methane, nitrous oxide, and nitric oxide in a moist tropical forest. Glob. Change Biol., 10, 718–730, doi: 10.1111/j.1529-8817.2003.00762.x, 2004.

Gut, A., S. M. van Dijk, M. Scheibe, U. Rummel, M. Welling, C. Ammann, F. X. Meixner, G. A. Kirkman, M. O. Andreae, and B. E. Lehmann, NO emission from an Amazonian rain forest soil: Continuous measurements of NO flux and soil concentration, J. Geophys. Res., 107(D20), 8057, doi:10.1029/2001JD000521, 2002.

Hanson, P. J., N. T. Edwards, C. T. Garten, and J. A. Andrews, Separating root and soil microbial contributions to soil respiration: a review of methods and observations, Biogeochemistry, 48(1), 115-146. 2000.

Hassler, E., Corre, M. D., Tjoa, A., Damris, M., Utami, S. R., and Veldkamp, E.: Soil fertility controls soil-atmosphere carbon dioxide and methane fluxes in a tropical landscape converted from lowland forest to rubber and oil palm plantations. Biogeosciences 12: 5831-5852. DOI: 10.5194/bg-12-5831-2015, 2015.

Holtgrieve, G. W., Jewett, P. K. and Matson, P. A.: Variations in soil N cycling and trace gas emissions in wet tropical forests. Oecologia, 146, 584–594, 2006.

Hricko, A.: Progress and pollution: port cities prepare for the Panama Canal expansion. Environ. Health Persp., 120, A470–32012, 2012.

Jacob, D. and Bakwin, P.: Cycling of NOx in tropical forest canopies, in: Microbial production and consumption of greenhouse gases: methane, nitrogen oxides and halomethanes, edited by: Rogers, J. E. and Whitman, W. B., American Society for Microbiology, Washington, DC, USA, 237–253, 1991.

Jenny, H.: Arrangement of soil series and types according to functions of soil-forming factors. Soil Sci., 61, 375–392, 1946.

Keller, M., and Reiners, W. A.: Soil-atmosphere exchange of nitrous oxide, nitric oxide, and

809 methane under secondary succession of pasture to forest in the Atlantic lowlands of Costa
810 Rica. Global Biogeochem. Cy., 8, 399–409, 1994.
811 Keller, M., Jacob, D. J., Wofsy S. C., and Harriss, R. C.: Effects of tropical deforestation on global
812 and regional atmospheric chemistry. Climatic Change, 19, 139–158, 1991.
813 Keller, M., Varner, R., Dias, J. D., Silva, H., Crill, P., de Oliveira, R. C., and Asner, G. P.: Soil–
814 atmosphere exchange of nitrous oxide, nitric oxide, methane, and carbon dioxide in logged
815 and undisturbed forest in the Tapajos national forest. Brazil, Earth Interact., 9, 1–28, 2005.
816 Kiese, R., Hewett, B., Graham, A., and Butterbach-Bahl, K.: Seasonal variability of N_2O and CH_4
817 uptake by tropical rainforest soils of Queensland, Australia. Global Biogeochem. Cy.,25
818 17, 1043, doi:10.1029/2002GB002014, 2003.
819 Koehler, B., Corre, M. D., Veldkamp, E., and Sueta, J. P.: Chronic nitrogen addition causes a
820 reduction in soil carbon dioxide efflux during the high stem-growth period in a tropical
821 montane forest but no response from a tropical lowland forest on a decadal time scale.
822 Biogeosciences, 6, 2973–2983, 2009a.
823 Koehler, B., Corre, M. D., Veldkamp, E., Wullaert. H., and Wright, S. J.: Immediate and long-
824 term nitrogen oxide emissions from tropical forest soils exposed to elevated nitrogen input.
825 Glob. Change Biol., 15, 2049–2066, 2009b.
826 Koehler, B., Zehe, E., Corre, M. D., and Veldkamp, E. An inverse analysis reveals limitations of
827 the soil- CO_2 profile method to calculate CO_2 production for well-structured soils.
828 Biogeosciences, 7: 2311–2325, 2010.
829 Koehler, B., Corre, M. D., Steger, K., Well, R., Zehe, E., Sueta, J. P. and Veldkamp, E. An in-
830 depth look into a tropical lowland forest soil: how 9-11 years experimental nitrogen
831 addition affected the contents of N_2O, CO_2 and CH_4 down to 2-m depth. Biogeochemistry

111: 695-713. Erratum in 111: 715-717, 2012.

Kursar, T. A.: Evaluation of soil respiration and soil CO_2 concentration in a lowland moist forest in Panama. Plant Soil, 113, 21–29, 1989.

Le Mer, J., and Roger, P.: Production, oxidation, emission and consumption of methane by soils: a review. Eur. J. Soil Biol., 37, 25–50, 2001.

Mariotti, A., Germon, J. C., Hubert, P., Kaiser, P., Letolle, R., Tardieux, A., and Tardieux, P.: Experimental determination of nitrogen kinetic isotope fractionation: some principles; illustration for the denitrification and nitrification processes. Plant Soil, 62, 413–430, 1981.

Mohanty, S. R., Bodelier, P. L. E., and Conrad, R.: Effect of temperature on composition of the methanotrophic community in rice field and forest soil. FEMS Microbiol. Ecol., 62, 24–31, 2007.

Nottingham, A. T., Turner, B. L., Winter, K., van der Heijden, M. G., and Tanner, E. V.: Arbuscular mycorrhizal mycelial respiration in a moist tropical forest. New Phytol., 186, 957-967, 2010.

Pape, L., Ammann, C., Nyfeler-Brunner, A., Spirig, C., Hens, K., and Meixner, F. X.: An automated dynamic chamber system for surface exchange measurement of non-reactive and reactive trace gases of grasslandecosystems. Biogeosciences, 6, 405-429, 2009.

Prather, M., Derwent, R., Ehhalt, D., Fraser, P., Sanhueza, E., and Zhou, X.: Other trace gases and atmospheric chemistry. In: Climate Change 1994 (eds Houghton JT, Meira Filho LG, Bruce J, Lee H, Callander BA, Haites E, Harris N, Maskell K), Cambridge University Press, Cambridge, UK, 73–126, 1995.

Pyke, C. R., Condit, R., Aguilar, S., and Lao, S.: Floristic composition across a climatic gradient in a neotropical lowland forest. J. Veg. Sci., 12, 553–566, 2001.

R Core Team. R: A language and environment for statistical computing. R Foundation for Statistical Computing, Vienna, Austria, ISBN 3-900051-07-0, URL: http://www.R-project.org/, 2013.

Raich, J. W., and Schlesinger, W. H.: The global carbon dioxide flux in soil respiration and relationship to vegetation and climate. Tellus, 44B, 81–99, 1992.

Rummel, U., C. Ammann, A. Gut, F. X. Meixner, and M. O. Andreae, Eddy covariance measurements of nitric oxide flux within an Amazonian rain forest, J. Geophys. Res., 107(D20), 8050, doi:10.1029/2001JD000520, 2002

Saikawa, E., Schlosser, C. A., and Prinn, R. G.: Global modeling of soil nitrous oxide emissions from natural processes. Global Biogeochem. Cy., 27, doi:10.1002/gbc.20087, 2013.

Santiago, L.S., Schuur, E.A. and Silvera, K.: Nutrient cycling and plant–soil feedbacks along a precipitation gradient in lowland Panama. J. Trop. Ecol., 21, 461–470, 2005.

Schwendenmann, L., and Veldkamp, E.: Long-term CO2 production from deeply weathered soils of a tropical rain forest: Evidence for a potential positive feedback to climate warming. Glob. Change Biol., 12, 1878–1893, 2006.

Schwendenmann, L., Veldkamp, E., Brenes, T., O'Brien J. J., and Mackensen, J.: Spatial and temporal variation in soil CO2 efflux in an old-growth neotropical rain forest, La Selva, Costa Rica. Biogeochemistry, 64, 111–128, 2003.

Silver, W.L., Neff, J., McGroddy, M., Veldkamp, E., Keller, M., and Cosme, R., Effects of Soil Texture on Belowground Carbon and Nutrient Storage in a Lowland Amazonian Forest Ecosystem. Ecosystems, 3, 193–209. doi:10.1007/s100210000019, 2000.

Silver, W. L., Thompson, A. W., McGroddy, M. E., Varner, R. K., Dias, J. D., Silva, H., Crill, P. M., and Keller, M.: Fine root dynamics and trace gas fluxes in two lowland tropical forest

878 soils. Glob. Change Biol., 11, 290–306, doi: 10.1111/j.1365-2486.2005.00903.x, 2005.
879 Sotta, E. D., Veldkamp, E., Guimaraes, B. R., Paixao, R. K., Ruivo, M. L. P., and Almeida, S. S.:
880 Landscape and climatic controls on spatial and temporal variation in soil CO2 efflux in an
881 Eastern Amazonian Rainforest, Caxiuana, Brazil. Forest Ecol. Manag., 237, 57–64, 2006.
882 Sotta, E. D., Corre, M. D., and Veldkamp, E.: Differing N status and N retention processes of soils
883 under old-growth lowland forest in Eastern Amazonia, Caxiuanã, Brazil. Soil Biol.
884 Biochem., 40, 740–750, 2008.
885 Sousa Neto, E., Carmo, J. B., Keller, M., Martins, S. C., Alves, L. F., Vieira, S. A., Piccolo, M.
886 C., Camargo, P., Couto, H. T. Z., Joly, C. A., and Martinelli, L. A.: Soil-atmosphere
887 exchange of nitrous oxide, methane and carbon dioxide in a gradient of elevation in the
888 coastal Brazilian Atlantic forest. Biogeosciences, 8, 733–742, doi:10.5194/bg-8-733-2011,
889 2011.
890 Sparks, J. P., Monson, R. K., Sparks, K. L., and Lerdau, M.: Leaf uptake of nitrogen dioxide (NO2)
891 in a tropical wet forest: Implications for tropospheric chemistry, Oecologia, 127(2), 214–
892 221, doi:10.1007/s004420000594, 2001.
893 Steudler, P. A., Melillo, J. M., Feigl, B. J., Neill, C., Piccolo, M. C., and Cerri., C. C.:
894 Consequences of forest-to-pasture conversion on CH4 fluxes in the Brazilian Amazon
895 Basin. J. Geophys. Res.-Atmos., 101, 18547–18554, doi:10.1029/96JD01551, 1996.
896 Stocker, T. F., Qin, D., Plattner, G. K., Tignor, M., Allen, S. K., Boschung, J., Nauels, A., Xia, Y.,
897 Bex, B., and Midgley, B. M.: IPCC, 2013: climate change 2013: the physical science basis.
898 Contribution of working group I to the fifth assessment report of the intergovernmental
899 panel on climate change. 2013.
900 Swaine MD. Rainfall and soil fertility as factors limiting forest species distributions in Ghana. J.

Ecol., 84, 419-428, 1996.

Tamai, N., Takenaka, C., Ishizuka, S., and Tezuka, T.: Methane flux and regulatory variables in soils of three equal-aged Japanese cypress (Chamaecyparis obtusa) forests in central Japan. Soil Biol. Biochem., 35, 633–641, 2003.

The World Factbook. https://www.cia.gov/library/publications/the-world-factbook/geos/pm.html [Accessed: March, 2015]

Townsend, A. R., Asner, G. P., and Cleveland, C. C.: The biogeochemical heterogeneity of tropical forests. Trends Ecol. Evol., 23, 424–431, 2008.

Turner, B. L., and Engelbrecht, B. M. J.: Soil organic phosphorus in lowland tropical rain forests. Biogeochemistry, 103, 295–315, 2011.

Veldkamp, E., B. Koehler, and M. D. Corre.: Indications of nitrogen-limited methane uptake in tropical forest soils. Biogeosciences 10, 5367–5379, 2013.

Verchot, L. V., Davidson, E. A., Cattânio, H., Ackerman, I. L., Erickson, H. E., and Keller, M.: Land use change and biogeochemical controls of nitrogen oxide emissions from soils in eastern Amazonia. Global Biogeochem. Cy., 13(1), 31–46, 1999.

Verchot, L. V., Davidson, E. A., Cattanio, J. H., and Ackerman, I. L.: Land-use change and biogeochemical controls of methane fluxes in soils of eastern Amazonia. Ecosystems, 3, 41–56, doi:10.1007/s100210000009, 2000.

Windsor, D. M.: Climate and moisture availability in a tropical forest, long term record for Barro Colorado Island, Panama. Smithson. Contrib. Earth Sci., 29, 1–145, 1990.

Wright, S. J., Yavitt, J. B., Wurzburger, N., Turner, B. L., Tanner, E. V., Sayer, E. J., Santiago, L. S., Kaspari, M., Hedin, L. O., Harms, K. E., Garcia, M. N., and Corre, M. D. Potassium, phosphorus, or nitrogen limit root allocation, tree growth, or litter production in a lowland

924 tropical forest. Ecology, 92, 1616–1625, 2011.
925 Yavitt, J. B., Wright, S. J., and Kelman Wieder, R.: Seasonal drought and dry-season irrigation
926 influence leaf-litter nutrients and soil enzymes in a moist, lowland forest in Panama.
927 Austral Ecol., 29, 177–188, 2004.
928 Zuur, A.F., Ieno, E.N., Walker, N.J., Saveliev, A.A., and Smith, G.M.: Mixed effects models and
929 extensions in ecology with R. Springer, New York., 2009.

930 **Table 1** Description of location, rainfall and geology of one hectare forest inventory plots located in the Panama Canal watershed,

931 central Panama.

Plot code [a]	Longitude, latitude	Elevation (m above sea level)	Forest age classification [a]	Soil taxonomic order [b]	Soil texture (% sand/ silt/clay) [c]	Precipitation (mm yr^{-1}) [b]	Geology [b]
Metropolitan	79º 33' W, 8º 59' N	30	mature secondary	Inceptisol (Cambisol)	3/35/62	1700	Aglomerate of andesitic tuff, Early-Late Oligocene
P27	79º 38' W, 9º 4' N	160	mature secondary	Inceptisol (Cambisol)	2/38/60	2030	Aglomerate of siltstone, tuff and limestone, Early Miocene
P8	79º 44' W, 9º 10' N	50	old growth	Oxisol (Ferralsol)	12/39/48	2360	Basaltic and andesitic lavas and tuff, pre-Tertiary
P19	79º 46' W, 9º 11' N	160	mature secondary	Oxisol (Ferralsol)	10/27/63	2690	Basaltic and andesitic lavas and tuff, pre-Tertiary
P32	79º 43' W, 9º 21' N	340	old growth	Oxisol (Ferralsol)	1/39/60	3400	Basaltic and andesitic lavas and tuff, pre-Tertiary

932 [a] Plot codes and forest age classification are from Pyke et al. (2001).

933 [b] Turner and Engelbrecht (2011) reported the tentative soil order (based on US Soil Taxonomy with equivalent FAO classification in

934 brackets), mean annual precipitation (estimated from location and elevation data as described by Engelbrecht et al. 2007), and the
935 geological information (taken from Stewart et al. 1980).
936 [c] Textural analyses are the weighted average of the sampling depth intervals: 0-5, 5-10, 10-25 and 25-50 cm.

Table 2 Soil biochemical characteristics in the top 50 cm of lowland forest soils along orthogonal gradients of annual precipitation (shown in brackets below each site) and soil fertility in the Panama Canal watershed, central Panama.

Soil characteristics [a]	Metropolitan (1700 mm)	P27 (2030 mm)	P8 (2360 mm)	P19 (2690 mm)	P32 (3400 mm)
$\delta^{15}N$ enrichment factor, ε [b]	-1.95 ± 0.52 [b]	-0.37 ± 1.69 [b]	-2.76 ± 0.54 [ab]	-4.70 ± 0.44 [a]	-2.65 ± 0.30 [ab]
$\delta^{15}N$ natural abundance (‰)	5.9 ± 0.8 [c]	6.3 ± 0.4 [bc]	12.0 ± 1.0 [a]	9.2 ± 0.9 [a]	7.0 ± 0.3 [b]
Organic C (mg C g^{-1})	12.8 ± 1.7 [ab]	10.8 ± 3.3 [b]	15.1 ± 0.2 [ab]	15.0 ± 1.3 [ab]	19.6 ± 2.1 [a]
Total N (mg C g^{-1})	1.08 ± 0.15 [b]	1.05 ± 0.25 [b]	1.49 ± 0.02 [ab]	1.44 ± 0.11 [ab]	1.85 ± 0.17 [a]
C:N ratio	10.9 ± 4.1 [a]	9.07 ± 1.8 [a]	9.76 ± 1.0 [a]	9.88 ± 1.0 [a]	10.1 ± 1.2 [a]
pH (1:4 H_2O)	6.20 ± 0.46 [a]	5.82 ± 0.72 [a]	5.05 ± 0.17 [b]	4.88 ± 0.30 [b]	5.14 ± 0.22 [b]
ECEC [c] ($mmol_c$ kg^{-1})	199 ± 72 [ab]	267 ± 11 [a]	56 ± 2 [c]	51 ± 6 [c]	118 ± 12 [bc]
Exch. bases [c] ($mmol_c$ kg^{-1})	198 ± 72 [a]	264 ± 10 [a]	37 ± 6 [c]	21 ± 8 [c]	90 ± 11 [b]
Exchangeable Al ($mmol_c$ kg^{-1})	0.22 ± 0.13 [b]	1.96 ± 0.51 [b]	12.2 ± 4.7 [ab]	22.6 ± 7.3 [a]	22.2 ± 3.2 [a]

[a] Means (±SE, n = 4) followed by different letters indicate significant differences between sites (one-way ANOVA with Tukey HSD at $P \leq 0.05$). Values for each replicate plot are weighted average of the sampling depth intervals of 0-5, 5-10, 10-25 and 25-50 cm.

[b] Calculated using Rayleigh equation (Mariotti et al. 1981): $\varepsilon = d_s - d_{so} / \ln f$; d_s- $\delta^{15}N$ natural abundance signatures at various depths in the soil profile, d_{so}- $\delta^{15}N$ natural abundance of the reference depth (top 5cm) and f is the remaining fraction of total N (i.e. total N concentration at a given depth divided by the total N concentration in the top 5 cm).

[c] ECEC – Effective cation exchange capacity; Exch. bases – sum of exchangeable Ca, Mg, K, Na

Table 3 Soil factors (measured in the top 5 cm of soil) and trace gas fluxes from lowland forest soils along orthogonal gradients of annual precipitation (mm per year; shown in brackets below each site) and soil fertility in the Panama Canal watershed, central Panama.

Site / season [a]	Soil temperature (° C)	Soil moisture ($g\ g^{-1}$)	Soil NH_4^+ ($mg\ N\ kg^{-1}$)	Soil NO_3^- ($mg\ N\ kg^{-1}$)	CO_2 flux ($mg\ C\ m^{-2}\ h^{-1}$)	CH_4 flux ($\mu g\ C\ m^{-2}\ h^{-1}$)	N_2O flux ($\mu g\ N\ m^{-2}\ h^{-1}$)	NO flux ($\mu g\ N\ m^{-2}\ h^{-1}$)
Wet season								
Metropolitan (1700)	25.8 (0.4)^{a}	0.64 (0.04)^{Ac}	5.94 (1.52)^{b}	1.95 (0.71)^{Ba}	126 (26)^{A}	1.47 (3.66)^{Aa}	5.78 (2.69)^{b}	-11.6 (7.08)^{Bb}
P27 (2030)	25.2 (0.4)^{b}	0.72 (0.06)^{Ab}	6.39 (1.35)^{Aab}	0.51 (0.17)^{Bc}	124 (18)^{A}	-3.01 (4.20)^{Aa}	4.15 (2.56)^{b}	-3.24 (2.68)^{Ba}
P8 (2360)	25.6 (0.4)^{Aab}	0.60 (0.03)^{Ac}	5.68 (0.94)^{ab}	1.32 (0.54)^{Bb}	131 (19)^{A}	-7.87 (6.95)^{Abc}	13.5 (7.0)^{Aa}	-3.95 (6.60)^{Ba}
P19 (2690)	25.5 (0.5)^{ab}	0.72 (0.06)^{Ab}	7.29 (1.39)^{ab}	0.46 (0.39)^{c}	129 (15)^{A}	-13.0 (6.92)^{Ac}	5.58 (3.13)^{Ab}	-3.98 (4.95)^{a}
P32 (3400)	24.6 (0.4)^{c}	0.90 (0.08)^{Aa}	8.21 (1.87)^{Aa}	0.49 (0.27)^{Bc}	107 (17)^{A}	-6.79 (6.09)^{Aab}	6.41 (3.09)^{b}	-4.01 (4.34)^{Ba}
Dry season								
Metropolitan (1700)	25.3 (0.3)^{a}	0.45 (0.06)^{Bb}	5.32 (1.26)^{bc}	3.42 (1.55)^{Aa}	82.7 (19)^{B}	-6.88 (4.14)^{Ba}	4.18 (4.62)	-4.05 (7.21)^{Aab}
P27 (2030)	24.7 (0.2)^{bc}	0.53 (0.08)^{Bab}	4.46 (0.89)^{Bc}	0.79 (0.18)^{Ab}	87.7 (14)^{B}	-12.1 (3.1)^{Bab}	4.87 (4.70)	1.09 (1.23)^{Aab}

P8 (2360)	24.9 (0.3)^{Bab}	0.48 (0.06)^{Bb}	6.04 (1.15)^{abc}	3.68 (1.16)^{Aa}	85.7 (17)^{B}	-21.3 (8.37)^{Bbc}	5.64 (5.75)^{B}	6.50 (3.76)^{Aa}
P19 (2690)	25.0 (0.3)^{ab}	0.49 (0.04)^{Bb}	7.47 (1.22)^{ab}	0.64 (0.26)^{b}	85.5 (12)^{B}	-29.2 (4.08)^{Bc}	1.30 (3.09)^{B}	-2.41 (2.35)^{b}
P32 (3400)	24.4 (0.3)^{c}	0.64 (0.09)^{Ba}	7.86 (1.37)^{a}	1.17 (0.61)^{Ab}	78.5 (15)^{B}	-17.4 (5.09)^{Bab}	5.89 (5.51)	4.34 (2.23)^{Aa}

[a] Means ((±SE, $n = 4$) followed by different lowercase letters indicate significant differences among sites within each season and different uppercase letters indicate significant differences between seasons within each site (linear mixed effects model with Tukey HSD test at $P \leq 0.05$).

Table 4 Annual[a] trace gas fluxes (mean (SE), n = 4) from lowland tropical forest soils along orthogonal gradients of annual precipitation and soil fertility in the Panama Canal watershed, central Panama.

Site (annual precipitation)	CO_2 (Mg C ha^{-1} yr^{-1})	CH_4 (kg C ha^{-1} yr^{-1})	N_2O (kg N ha^{-1} yr^{-1})	NO (kg N ha^{-1} yr^{-1})
Met (1700 mm)	8.48 (0.70)	-0.34 (0.17)	0.41 (0.06)	-0.82 (0.16)
P27 (2030 mm)	9.16 (0.62)	-0.51 (0.04)	0.43 (0.06)	-0.12 (0.04)
P8 (2360 mm)	10.14 (0.76)	-1.45 (0.15)	1.07 (0.15)	-0.17 (0.17)
P19 (2690 mm)	9.89 (0.49)	-1.98 (0.07)	0.35 (0.05)	-0.21 (0.10)
P32 (3400 mm)	7.89 (0.84)	-0.94 (0.19)	0.66 (0.18)	-0.03 (0.09)

[a] Calculated using the trapezoidal rule between fluxes and time interval, covering the measurement periods of January - December 2011 for CO_2 , CH_4 and N_2O, and June 2010 - May 2011 for NO. Annual fluxes were not tested statically for differences among sites since these are trapezoidal extrapolations.

Formatted Table
Formatted: Centered
Formatted: Centered
Formatted: Centered
Formatted: Centered
Formatted: Centered

Table 5 Spearman correlations of soil biochemical characteristics[a] and annual (measured in 2011) soil trace gas fluxes from five lowland tropical forests along orthogonal precipitation and fertility gradients in the Panama Canal watershed, central Panama.

	ECEC	BS	Na	Al	pH	Clay	CO_2	CH_4	N_2O	NO
^{15}N sig.	-0.87**	-0.67**	-0.30	0.42	-0.61**	-0.15	0.41	-0.70**	0.30	0.16
ECEC		0.80**	0.34	-0.50	0.76**	-0.12	-0.33	0.77**	-0.09	-0.17
BS			-0.13	-0.87**	0.96**	-0.12	-0.40	0.78**	-0.12	-0.54
Na				0.45	-0.18	-0.15	0.04	0.01	-0.01	0.60**
Al					-0.87**	0.04	0.24	-0.71**	0.17	0.58**
pH						-0.04	-0.34	0.76**	-0.12	-0.54
Clay							-0.13	-0.17	-0.67**	-0.34
CO_2								-0.24	0.26	0.10
CH_4									-0.07	-0.31
N_2O										0.19

** $P < 0.01$, $n = 20$ (4 replicate plots in each of the 5 forest sites)

[a] Soil parameter abbreviations: ^{15}N natural abundance signature (^{15}N sig.), effective cation exchange capacity (ECEC) and base saturation (BS).

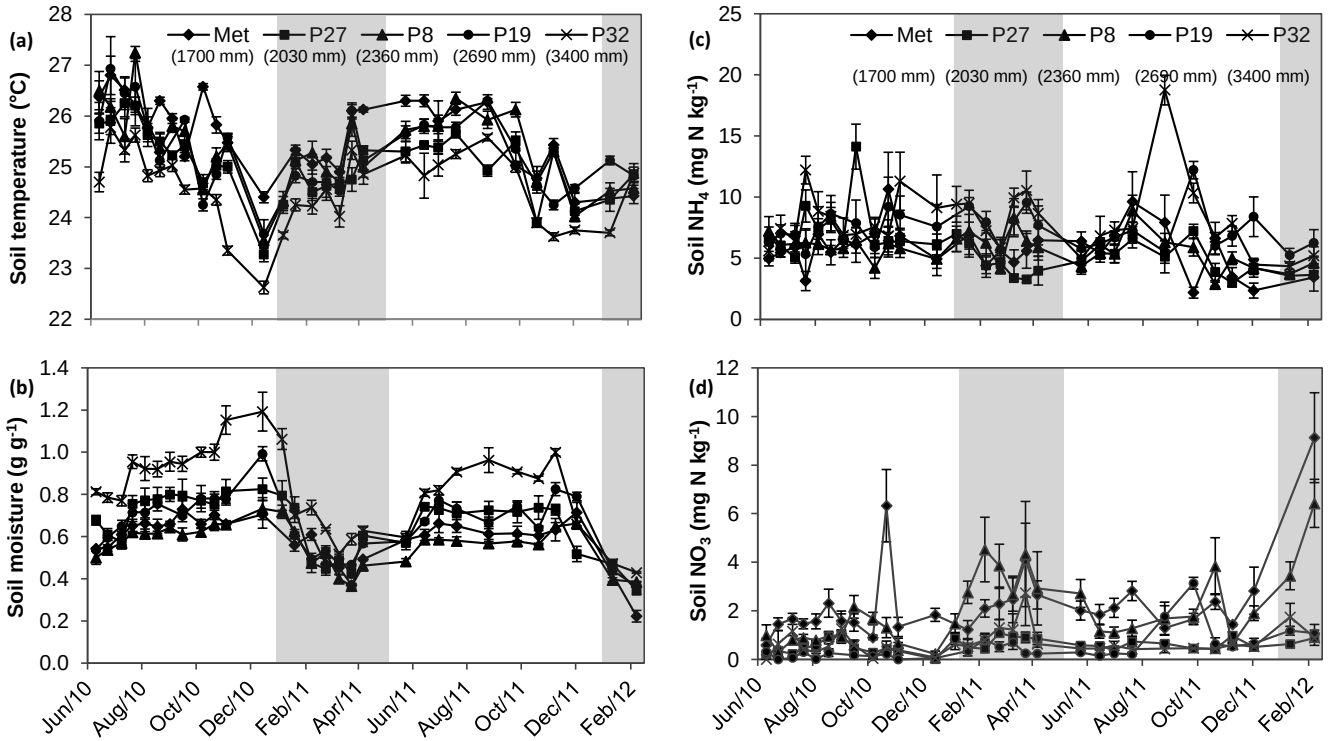

Fig. 1 Mean (±SE, n = 4) soil **(a)** temperature, **(b)** moisture, **(c)** NH_4^+ and **(d)** NO_3^- concentrations measured in the top 5 cm of soil in lowland forests along orthogonal gradients of annual precipitation and soil fertility in the Panama Canal watershed, central Panama. Gray shading indicates the dry season (January through April).

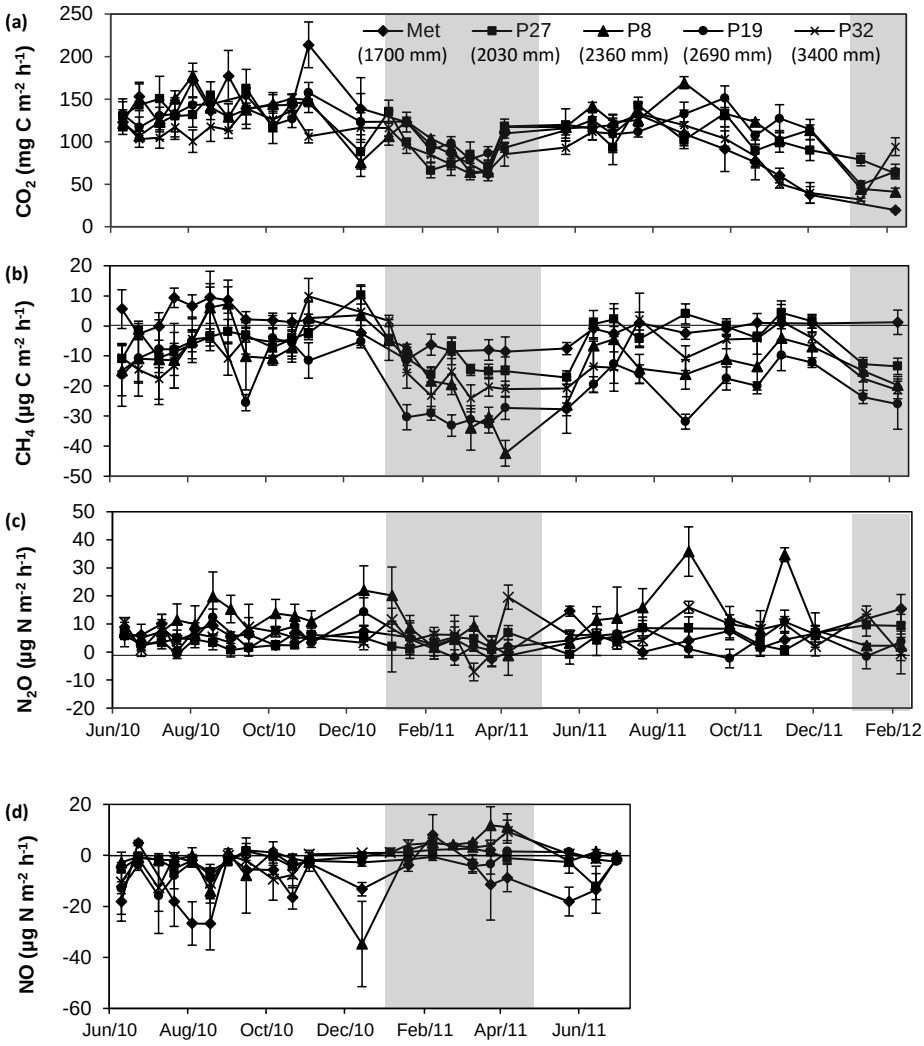

Fig. 2 Mean (±SE, n = 4) soil **(a)** CO_2, **(b)** CH_4, **(c)** N_2O and **(d)** NO fluxes from lowland forests along orthogonal gradients of annual precipitation and soil fertility in the Panama Canal watershed, central Panama. Gray shading indicates the dry season (January through April).

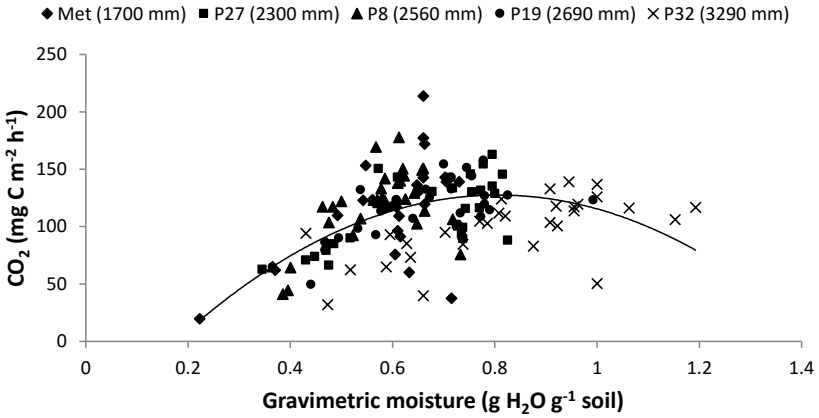

Fig. 3 Soil CO_2 fluxes and moisture contents (top 5 cm) in five lowland forests along orthogonal gradients of annual precipitation (shown in brackets) and soil fertility in the Panama Canal watershed, central Panama. Each data point is the average of four replicate plots on one sampling day from one of the five sites, measured from June 2010 to February 2012 ~~(n = 145)~~; the quadratic regression across sites (shown) is: $y = -321.1x^2 + 517.8x - 81.2$ ($R^2 = 0.30$, $n = 145$, $P<0.01$).

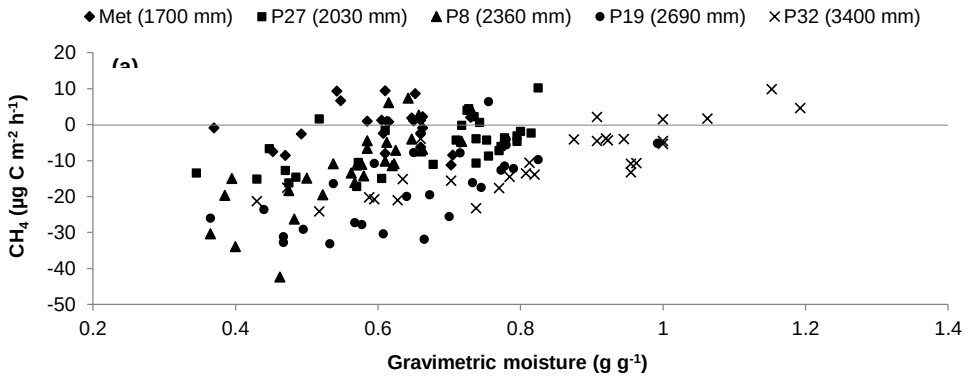
Met (1700 mm)
P27 (2030 mm)
P8 (2360 mm)
P19 (2690 mm)
P32 (3400 mm)
(a)
CH4 (µg C m-2 h-1)
Gravimetric moisture (g g-1)

39

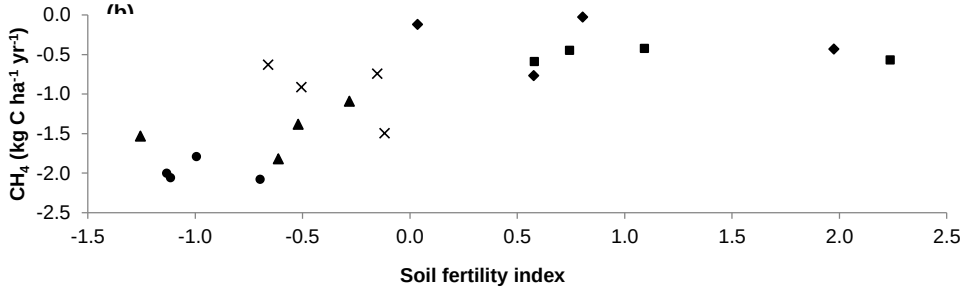
(b)
CH4 (kg C ha-1 yr-1)
Soil fertility index

40

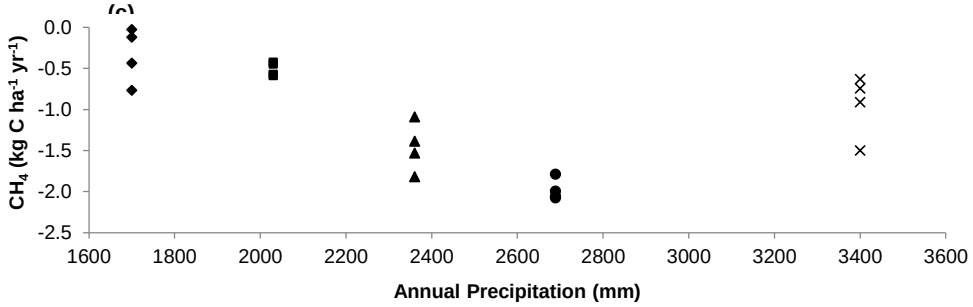
(c)
CH4 (kg C ha-1 yr-1)
Annual Precipitation (mm)

41

Fig. 4 Average daily soil CH_4 fluxes plotted against (a) soil moisture (top 5 cm), and annual soil CH_4 fluxes plotted against (b) soil fertility index and (c) annual precipitation. For (a), each data point is the average of four replicate plots on each sampling day of each of the five sites, measured from June 2010 to February 2012. The five lowland forests are located along orthogonal gradients of annual precipitation and soil fertility in the Panama Canal watershed, central Panama.

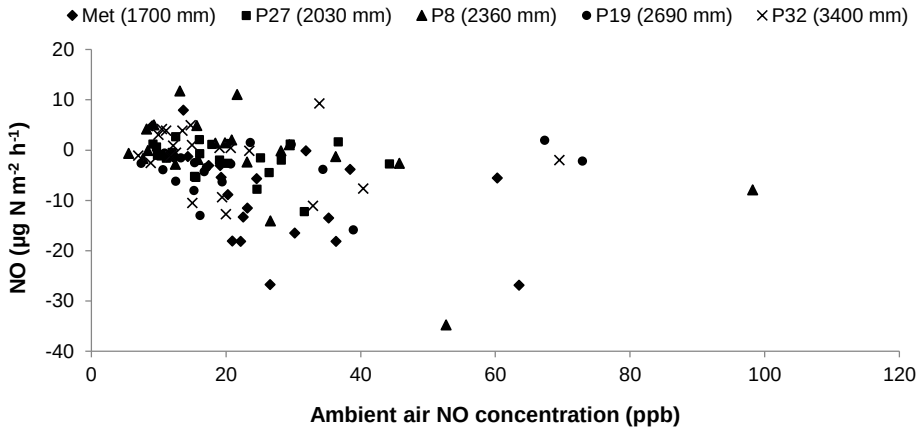

Fig. 5 Soil NO fluxes plotted against ambient air NO concentrations; each data point is the average of four replicate plots on each sampling day in each of the five sites, measured from June 2010 to June 2011. The five lowland forests are located along orthogonal gradients of annual precipitation and soil fertility in the Panama Canal watershed, central Panama.